ACS Sustainable Chemistry & Engineering

pubs.acs.org/journal/ascecg

Research Article

A Greener Chemistry Process Using Microwaves in Continuous Flow to Synthesize Metallic Bismuth Nanoparticles

Gauthier Hallot, Virginie Cagan, Sophie Laurent, Catherine Gomez,* and Marc Port*

Cite This: *ACS Sustainable Chem. Eng.* 2021, 9, 9177−9187

Read Online

ACCESS | Metrics & More | Article Recommendations | Supporting Information

ABSTRACT: To address environmental concerns, improving synthesis processes in the nanoparticle field was a major challenge. Several processes of bismuth nanoparticle synthesis have been proposed in the past 10 years, but none of them have answered to all green chemistry principles suitable for nanomaterials. In this work, two syntheses of bismuth nanoparticles involving conventional thermal heating and microwave irradiation were compared in batch. All parameters have been studied to optimize the size and distribution of metallic bismuth nanoparticles. The choice of precursor, reducing agent, coating agent, solvents, the evaluation of quantities and the follow-up of reduction step, never documented before, have been fully described in this work. Following this optimization, the validation of synthesis reproducibility confirmed that microwave irradiation was the best process for obtaining bismuth nanoparticles according to green chemistry criteria. This study was continued using a millifluidic process to increase productivity. This continuous flow synthesis under microwave irradiation responded to industrial challenges and provided access to monodisperse bismuth nanoparticles that were characterized by several techniques.

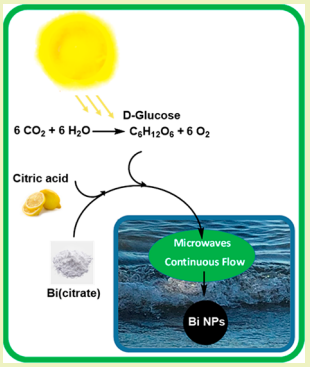

KEYWORDS: *green nanochemistry, continuous flow, microwaves, bismuth, reproducibility*

INTRODUCTION

Huge progress in nanotechnology research and development now makes it possible to produce nanomaterials with unprecedented properties, enabling access to new applications in many industrial fields, especially in the biomedical field.[1] However, the impact on the environment and the health of new nanoparticle production remains a major challenge. To answer this challenge, the concept of green nanotechnology has been proposed by applying the green chemistry principles to nanoparticle synthesis across the nanoproduct lifetime.[2−4]

Over the past years, metallic bismuth nanoparticles (NPs) have attracted great attention due to their interesting properties. Bismuth is a diamagnetic semimetal with a very small band gap. This material shows several properties such as high magnetoresistance, thermal conductivity, and high anisotropic electronic behavior.[5] In the literature, electronic applications showed that bismuth could transfer from a semimetal to a semiconductor because the bismuth NPs size is decreased. This property is linked to quantum confinement, which gives a thermoelectric efficiency at room temperature.[6] Bismuth NPs are also studied as chemical catalysts to reduce nitrobenzene to azobenzene.[7] On the other hand, Cui et al. have characterized bismuth NPs photocatalytic activity.[8] Finally, several recent works have shown the interest of bismuth NPs in medical applications,[9] especially as antimicrobial agents, as contrast agents in X-ray imaging[10−14] or in photoacoustic imaging,[15−18] and as radiosensitizers that can potentiate radiotherapy[19−25] or thermotherapy.[15−18,24,26,27] In view of many advantages and different applications of metallic bismuth, the development of a new process to synthesize these nanoparticles is considered in this work. Our strategy has been developed with respect to all settings established in greener nanoparticle preparation.[28,29] Indeed, in the published articles mentioning metallic bismuth NPs syntheses, which have been reviewed and critically discussed, no synthesis is known in light of the six principles of new nanomaterial design.[30] Recently, we have optimized and made a reliable and reproductive synthesis of bismuth NPs by sonochemistry that is partially green. However, this synthesis still uses an organic solvent (1,2-propanediol) and, especially, a toxic reducer (borane morpholine).

This encouraged us to design a new way of bismuth NPs synthesis that respects all the six principles of new nanomaterials design.

To do this, we have engineered a synthesis that must consider the following criteria:

- Do not use an organic solvent but water as a green solvent.

Received: January 19, 2021
Revised: June 10, 2021
Published: July 6, 2021

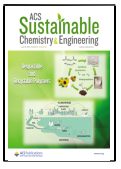

https://doi.org/10.1021/acssuschemeng.1c00396
ACS Sustainable Chem. Eng. 2021, 9, 9177−9187

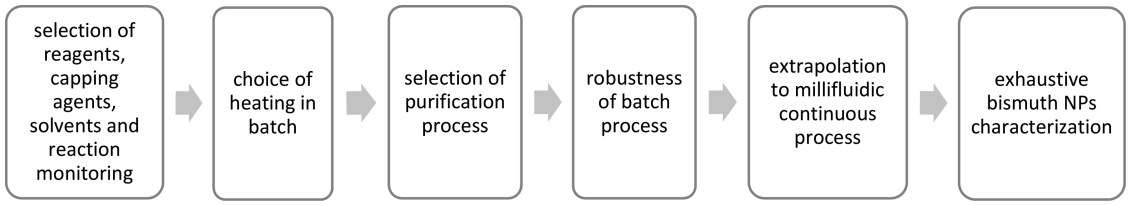

Figure 1. Research program to develop a greener bismuth NPs synthesis process.

Table 1. Solubility of Bi(III) Salts at pH = 14 (Ac, acetate; Cit, citrate)

Bi(III) salt @ 10 mM	$BiCl_3$	$BiAc_3$	$Bi(NO_3)_3$	$Bi_2(CO_3)_3$	$[(NH_3)_3Bi(Cit)_2]$	NaBiCit
solubility at pH 14	insoluble	insoluble	insoluble	insoluble	soluble	soluble

- Do not use toxic reducers such as sodium borohydride[31] and hydrazine hydrate[32] but, on the contrary, use a feedstock renewable reducer, D-glucose.[33]
- Use water-soluble precursors to consider synthesis in flow millifluidic systems.
- Do not require a high energy input (unlike top-down methods, thermal decomposition, or polyol synthesis).
- Minimize the excess of reactants and use capping agents based on renewable feedstock such as citrate.
- Limit waste reduction at the synthesis step but especially in the purification step.

To achieve this optimization, the choice of precursors (bismuth sources and reducer), reaction conditions, activation method (thermal versus microwaves),[34] and purification will be studied.

All the advantages of our batch procedure and their influence on the size and distribution of nanoparticles will be highlighted. Finally, to increase bismuth NP productivity, the extrapolation of batch to flow chemistry conditions will be demonstrated and then bismuth NPs obtained will be characterized in detail.

Taking into account all these reaction parameters, this work proposes and discusses a simple, efficient, robust, and reproducible synthesis to obtain bismuth NPs according to a greener process.

RESULTS AND DISCUSSION

A new research strategy to develop greener and optimized conditions has been developed to synthesize metallic bismuth NPs that can be extrapolated into a millifluidic continuous process.

Our research approach has been conceptualized to develop a bismuth NP synthesis that fully respects the green chemistry principles. This work has been organized as follows (Figure 1):

(i) The choice of the solvent, the reducing agent, and the capping agent employed to select environmentally friendly and safe reactants.
(ii) The choice of a heating system to reduce the energy requirements and to ensure the synthesis reproducibility: conventional heating system or microwave system.
(iii) The selection of a productive and reproducible purification process.
(iv) The robustness of the batch process. Indeed, in the field of metallic nanoparticle synthesis, it is essential to ensure the reproducibility of results as we have already shown in previous publications.[28,29]
(v) The extrapolation of the batch process to the millifluidic continuous process. Indeed, the use of millifluidic continuous operating systems is tremendous to produce valuable chemical nanoparticles in the scale-up.[35,36]
(vi) The exhaustive characterization of produced bismuth NPs.

Bismuth NPs Synthesis in the Batch Process.

Selection of Reagents, Solvents, and Reaction Monitoring. To establish a greener bismuth NPs preparation, first, water is selected as a solvent.[37] Indeed, water is a green solvent (it is interesting to get rid of the organic solvent in the perspective of the medical use of bismuth NPs) and residues of organic solvents may pose problems in terms of toxicology.[38] It should be emphasized that few syntheses of metallic bismuth NPs are described in an aqueous medium.[30]

This choice is not without consequences since the use of both a water-soluble precursor of Bi(III) and a nontoxic water-soluble reducing agent is required.

Some water-soluble reducing agents such as citric acid,[39] ascorbic acid,[8] or D-glucose[40] have been used in the literature, particularly for metallic gold nanoparticle synthesis. Our choice stopped on D-glucose because this compound is nontoxic, bio-sourced and is thus perfectly compatible with a green synthesis. In the literature describing bismuth NPs synthesis, D-glucose has never been used as a reducing agent but only as a coating agent to stabilize the nanoparticles.[11]

The reducing power of D-glucose depends on the pH of the solution.[40] The Pourbaix diagram shows that the reducing power of D-glucose is higher at a basic pH.[40] Not knowing *a priori* the oxidation-reducing potentials of different Bi(III) salts, the pH is set at 14 to maximize the reducing capacity of D-glucose.

In order to minimize mixing problems and avoid the use of heterogeneous conditions, which can cause potential difficulties in terms of reproducibility and are unfavorable for further millifluidic extrapolation, several bismuth(III) salts were tested at pH = 14. The solubility screening is evaluated by visual inspection after 1 h (Table 1).

The only two soluble Bi(III) salts at pH 14 are bismuth ammonium citrate and sodium bismuth citrate. The sodium bismuth citrate precursor was chosen instead of bismuth ammonium citrate to maximize atom economy (absence of an ammonium cation). In addition, the citrate counter-ion can act as a coating agent for the nanoparticle. Finally, citrate can be bio-sourced from *Yarrowia lipolytica* bacteria,[41] which adds benefit in terms of green chemistry.

The use of water as a solvent also allows us to monitor the reduction of Bi(III) to Bi(0) by a pH measurement. Indeed,

https://doi.org/10.1021/acssuschemeng.1c00396
ACS Sustainable Chem. Eng. 2021, 9, 9177−9187

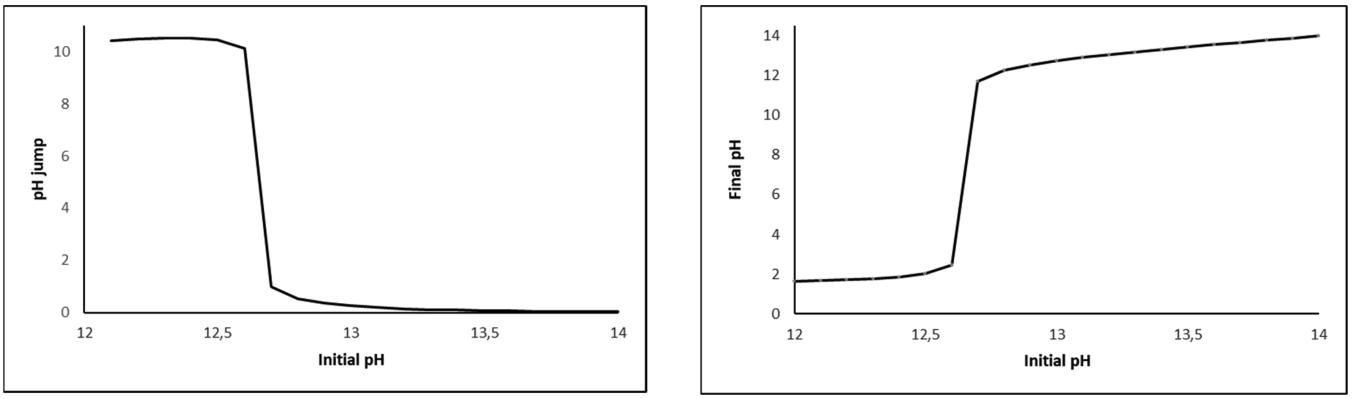

Figure 2. Theoretical pH jump for a total reduction of Bi(III) to Bi(0) (final pH) (left). Final pH calculated from initial pH and initial Bi(III) concentration (10 mM) (right).

the reduction of Bi(III) by D-glucose is described by the following redox equations (eqs 1−3):

Reduction of Bi(III) by D-Glucose [Bi(III)]

$$Bi^{3+} + 3\,e^- \longrightarrow Bi^0 \quad (1)$$

$$\text{Glucose} + 3\,OH^- \longrightarrow \text{gluconate} + 2\,H_2O + 2e^- \quad (2)$$

$$1\,Bi^{3+} + 1.5\,\text{Glucose} + 4.5\,OH^- \longrightarrow 1\,Bi^0 + 1.5\,\text{gluconate} + 3\,H_2O \quad (3)$$

These equations show that the total reduction of Bi(III) to Bi(0) requires a stoichiometric ratio of D-glucose/Bi(III) of 1.5 and is accompanied by a consumption of 4.5 hydroxide ions, leading to a pH decrease. Accordingly, a simple measurement of the pH change during the reaction can be used to monitor the reduction and evaluate the reaction conversion.

The final theoretical pH, corresponding to a total reduction of Bi(III) to Bi(0), is a function of bismuth concentration. The final pH is evaluated *via* the following equation in the function of the $pH_{initial}$ (eq 4).

Calculation of Final pH from the Bi(III) Concentration according to $pH_{initial}$

$$\text{pH final} = -\log\left[\frac{10^{-14}}{\frac{10^{-14}}{10^{-pH_{initial}}} - 4.5 \times [\text{Bi(III)}]}\right] \quad (4)$$

In the batch experiment, the initial Bi(III) concentration was fixed at 10 mM. Under these conditions, a sudden jump ΔpH is deduced from eq 4 for a $pH_{initial}$ of 12.7. Indeed, under a $pH_{initial}$ of 12.7, all the OH^- ions of the basic solution are consumed to completely reduce 10 mM Bi(III) (Figure 2).

The calculated data in Figure 2 (left) show that the initial pH should not be reduced below 12.7 to avoid a significant and brutal acidification. Indeed, at acid pH values (pH < 5), bismuth NPs are degraded by acidic dissolution (data not shown). Therefore, the pH range usable in our synthesis is set at 12.7 < pH < 14 to ensure a basic final pH to manage the stability of bismuth NPs. As previously mentioned, our first experiments are carried out starting from an initial pH fixed at 14 to benefit from the maximum reducing power of D-glucose, even if at this pH, the jump of pH allowing one to monitor the reaction is weak (ΔpH = 0.03).

Selection of Heating in Batch. Following the selection of reagents and the solvent to respect the principles of green chemistry, we carried out preliminary reaction in batch using a conventional thermal heating and a purification using the centrifugation technique (Scheme 1 and Table 2).

Scheme 1. Conditions of Bismuth NPs Synthesis by Conventional Thermal Heating

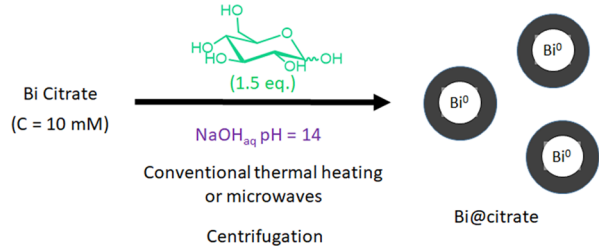

Table 2. Sizes of Bismuth NPs Obtained by Different Activation Methods (Purification by Centrifugation)

activation	reaction time	sizes (nm) in number (proportions %)
conventional thermal heating (120 °C)	2 h 30 min	94 ± 22 (65%) 222 ± 89 (35%)
microwaves (120 °C)	1 min	924 ± 201 (62%) 283 ± 46 (38%)

In addition to monitoring the pH jump, the formation of nanoparticles is followed visually (appearance of a black coloration) and by measuring the hydrodynamic diameter with DLS (expressed in number).

This preliminary study allowed to demonstrate that our reaction conditions completely reduce Bi(III) to Bi(0) (complete pH jump = 0.03) with D-glucose at pH 14. A minimum temperature of 120 °C and a time reaction of 2 h 30 min have been necessary to obtain a black solution of bismuth NPs characterized by bimodal size distributions of 94 ± 22 nm (65%) and 222 ± 89 nm (35%) (Table 2). These first preliminary results were very interesting and highlighted new greener conditions to obtain bismuth NPs in aqueous conditions with nontoxic precursors and reagents.

However, these results had to be optimized because the bismuth NPs obtained were polydisperse in DLS and also the reaction conditions used were not completely ideal from the point of green chemistry view with a hourly productivity limited to 6 mg. Especially in terms of safety and energy consumption, the high temperature (required a sealed tube)

https://doi.org/10.1021/acssuschemeng.1c00396
ACS Sustainable Chem. Eng. 2021, 9, 9177−9187

and the long reaction time implied an important energy consumption (Table S1).

To overcome these drawbacks and develop a greener synthesis, we have considered replacing the conventional thermal heating by the use of microwave. It is indeed well known that microwave heating[42] not only reduces the chemical reaction times by several orders of magnitude (and consequently minimizes the energetic need related to the reaction) but also improves the yield of nanoparticle synthesis.[43−45] In addition, it is important to select reaction conditions such as mixing (mass transport) and heating (heat transport), which can be controlled very precisely to achieve good reproducibility in terms of size distribution of nanoparticles.[46] Indeed, inhomogeneities in the growth process can be amplified by thermal gradients in the reaction mixture, thus producing poor nucleation processes and consequently broad size distributions. In this regard, dielectric volumetric heating brought by microwaves, which is able to heat a reaction mixture very homogeneously and very rapidly, should provide interesting conditions for the preparation of monodisperse nanoparticles.[47] Finally, beyond the efficient internal heating and the corresponding acceleration of reaction kinetics (dissolution of precursor, nucleation, and growth), microwaves can have additional effects influencing the properties of the nanoparticles obtained such as the selective heating or nonthermal effect even if the existence of these effects is not clearly demonstrated and is still the subject of scientific controversy.[48,49]

To our knowledge, several methods of metallic nanoparticles synthesis under microwave irradiation have been proposed in the literature,[50−55] but only four publications described the use of microwaves to produce bismuth NPs.[8,56−58] All these publications used the polyol route where polyol acts as both a polar solvent and a reducing agent. However, in these publications, the irradiation conditions have often been described on domestic microwave ovens and a lack of specific information due to an approximate description of power, reaction temperature, and pressure has been identified concerning the metallic nanoparticles synthesis. To our knowledge, no synthesis of bismuth NPs in water as a solvent activated by an alternative energy-input system, such as microwaves, has been described. Water is classified as a medium microwave-absorbing solvent with a tan δ of 0.123.[48,49] However, the addition of polar reagents such as D-glucose and citrate could increase the absorbance level of our reaction medium.

In a microwave batch study, two modes of microwave device use were tested: dynamic mode and power fixed mode. In dynamic mode, the temperature was kept constant at 120 °C to compare the results to those obtained in conventional thermal heating conditions.

A total reduction of Bi(III) to Bi(0) (complete pH jump) was obtained in 1 min, confirming the acceleration of kinetics by microwaves. However, bismuth NPs sizes were much larger than those obtained with conventional thermal heating (Table 2).

Thus, the comparison between the conventional heating and the "dynamic" mode with a fixed temperature was not attractive as these conditions induce the aggregation of bismuth NPs.

The second microwave mode, "power fixed" mode, was tested to compare the influence of microwave power on the size and polydispersity of bismuth NPs. In the few works using microwave irradiation to prepare bismuth NPs, all used this fixed power mode in reference to domestic microwave ovens previously used.

The reaction time was determined by pH monitoring to obtain a complete pH jump, indicating the total reduction of Bi(III) salts to Bi(0) species.

At a high power of 100 W, a monodisperse population of large size is observed to be relevant to bismuth NPs aggregates (Table 3, entry 1). At a lower power (50 W), polydispersed nanoparticles (three size populations) are isolated over a longer time of 3 min 30 sec (Table 3, entry 3). The most interesting results are obtained at 75 W after 2 min 10 sec of microwave irradiation (Table 3, entry 2), less energy consumption compared to conventional thermal heating (Table S1).

Table 3. Experimental Conditions under Microwave Irradiation in Power Fixed Mode (Purification by Centrifugation)

entry	reaction time[a]	power	sizes (nm) in number (proportions %)
1	2 min	100 W	757 ± 158 (100%)
2	2 min 10 sec	75 W	115 ± 34 (82%)
			315 ± 87 (17%)
3	3 min 30 sec	50 W	122 ± 16 (15%)
			196 ± 39 (30%)
			476 ± 248 (55%)

[a]Time to achieve a complete pH jump.

Under these last conditions, a bimodal distribution in size is obtained quite comparable to conventional thermal heating (Table 2) but in a shorter reaction time (two orders of magnitude).

Selection of the Purification Process. For all these first small-scale experiments, bismuth NPs are purified by centrifugation, a technique very frequently used in the literature for bismuth NPs.[30] To consider a scale-up, we used an experimental ultrafiltration device that is a faster, safer, and more productive purification system in comparison to centrifugation.[28,29]

These two purification methods (centrifugation and ultrafiltration) were compared (Table 4) on the same batch of bismuth NPs obtained in our best microwave conditions (Table 3, entry 2).

Table 4. Sizes of Bismuth NPs Purified by Centrifugation or Ultrafiltration

purification method	sizes (nm) in number (proportions %)
successive centrifugations (×3) at 4000 rpm	115 ± 34 (82%)
	315 ± 87 (17%)
ultrafiltration on regenerated cellulose filter (5 kDa)	115 ± 31 (100%)

The removal of low-molecular-weight species such as salts, gluconate, and sodium citrate was followed by conductimetry measurement of the supernatant for centrifugation and the filtrate for ultrafiltration.

A similar main hydrodynamic diameter of 115 nm is obtained for both purification techniques, but very interestingly, after ultrafiltration, the monodispersity of bismuth NPs is improved with a monomodal distribution in DLS. The

https://doi.org/10.1021/acssuschemeng.1c00396
ACS Sustainable Chem. Eng. 2021, 9, 9177−9187

centrifugation technique likely induces bismuth NPs aggregation when these are concentrated in the pellet of the centrifuge tube. Therefore, in our view of green chemistry, ultrafiltration is very interesting because it allows rapid, safer, and efficient purification and also allows obtaining bismuth NPs of uniform sizes without inducing their aggregation unlike centrifugation.

Reproducibility and Repeatability. To confirm the potential of bismuth NPs synthesis and purification conditions, an intra- and inter-operator reproducibility study is performed (Scheme 2). The bismuth yield of our experiments

Scheme 2. Batch Synthesis Conditions of Bismuth NPs under Microwave Irradiation

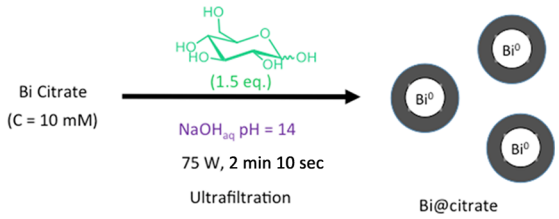

is also evaluated *via* a bismuth NPs digestion protocol followed by a colorimetric assay of the digested bismuth (see Experimental Section) (Table 5).

Table 5. Intra- and Inter-operator Reproducibility of Bismuth NPs Synthesis under Microwave Irradiation in Power Fixed Mode

operator	number of test	average sizes (nm) in number (average proportions %)	yield after ultrafiltration purification
A	9	113 ± 40 (100%)	72%
B	3	127 ± 30 (100%)	74%

The obtained bismuth yields after purification by ultrafiltration were only in the order of 72−74%, which demonstrated a loss of around 25% in the purification step (as the total reduction of Bi(III) observed thanks to the pH jump). Moreover, the intra- and inter-operator reproducibility was excellent, demonstrating the viability of both synthesis conditions and the ultrafiltration purification system.

Stability Study of Bismuth NPs. The stability of bismuth NPs in aqueous solution at a concentration of 1 mM was then studied by sedimentation time evaluation with a visual observation. Bismuth NPs resulting from our reproducibility study were stable for 15 min (Table 6, entry 1).

In an attempt to increase the stability, we modified the following (Table 6):

Table 6. Sedimentation Time of Bismuth NPs Prepared at Initial pH 13 or 14 Formulated or Not with 10 equiv of Citrate

entry	initial pH of synthesis	added citrate (equiv)	sedimentation time (min)	sizes (nm) in number (proportions %)
1	14	0	15	113 ± 40 (100%)
2	14	10	45	113 ± 63 (100%)
3	13	0	60	141 ± 80 (100%)
4	13	10	180	96 ± 37 (100%)

- The formulation of bismuth NPs with an excess of citrate. After adding the citrate, the solution is activated for 1 min under microwave irradiation at 75 W.
- The initial pH of the reaction at the value of 13. This pH decrease has been considered to better control the pH jump (Figure 2) and to anticipate a switch from batch to millifluidic syntheses with less aggressive conditions for the HPLC device.

The formulation with an excess of citrate stabilized the bismuth NPs (Table 6, entries 2 and 4). Remarkably, the modification of the initial pH at 13 also induced a stabilization of bismuth NPs (Table 6, entries 3 and 4). The effect was synergistic since the most stable bismuth NPs were those synthesized at pH = 13 with a formulation containing 10 equiv of sodium citrate (Table 6, entry 4).

Productivity Increase of Bismuth NPs in Green Conditions. These first results obtained in batch using microwaves were interesting thanks to the sizes and reproducibility obtained. Nevertheless, the productivity of these experiments remained low: 40 mg/h of bismuth NPs per batch. To improve this productivity, our conditions were transposed from batch to a continuous millifluidic flow process. As mentioned previously, obtaining monodisperse NPs depends on the quality of the heat and mass transfers in the selected process.[40] In this perspective, to simultaneously optimize the heat and mass transfers, the coupling of continuous flow[36] and microwave seems ideal[59−64] and responds to current industrial challenges.[65]

Moreover, the use of a continuous millifluidic flow process makes it possible to satisfy the two criteria of green chemistry, "inherently safer chemistry for accident prevention" and "less hazardous chemical syntheses", using a process at pH 13. Millifluidic chemistry is becoming a strategic tool for carrying out hazardous chemical reactions more safely and for optimizing the safety of a chemical process.[66,67] This basic pH is compatible with all millifluidic systems, which can be manufactured to avoid corrosion problems. Indeed, HPLC pumps or peristaltic pumps can be made entirely metal-free (PTFE), plungers and seals can also be made of silicon carbide, which is resistant to very harsh conditions. In addition, commercial millifluidic systems, such as Corning G1 SiC, are suitable for an industrial scale-up and can operate at a basic pH.[68]

Synthesis of Bismuth NPs. For that purpose, a millifluidic setup is designed with an HLPC pump (an adjustable flow rate between 1 and 2 mL/min) to inject the reaction mixture in a Teflon tubing heated by microwaves (Figure 3). The millifluidic system is inspired from the literature[69] and is made of a Teflon cylinder that holds the Teflon tubing. To ensure the maximum absorption of microwaves, the tubing diameter (3.2 mm) is chosen to be much lower than the depth of microwave penetration in water (a few centimeters). Bismuth NPs synthesized are cooled at room temperature at the exit of the reactor and then collected. Preliminary experiments have shown the need of a flow rate regulator at the output of the experimental device to regulate the flow rate inside the reactor (Figure 3).

The reaction conditions used in flow are directly extrapolated from our batch work and the purification is carried out by ultrafiltration. The pH is lowered to pH 13 to better control the pH jump (Figure 2) and to work under less aggressive conditions for the HPLC material. To ensure a

https://doi.org/10.1021/acssuschemeng.1c00396
ACS Sustainable Chem. Eng. 2021, 9, 9177−9187

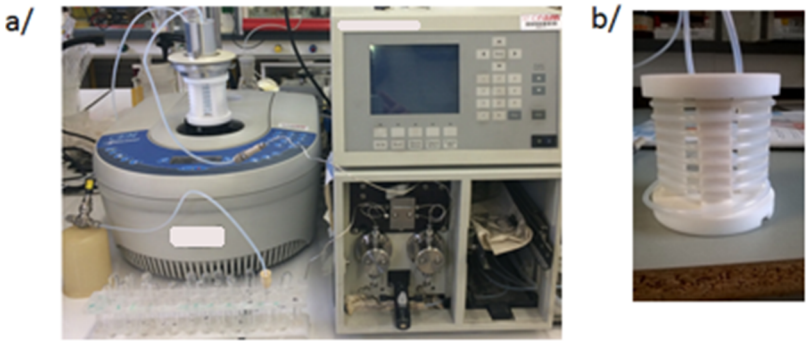

Figure 3. (a) Photograph of the millifluidic system under microwaves. (b) Photograph of the reactor with Teflon tubing.

complete pH jump and, thus, a total reduction of Bi(III), 3 equiv of D-glucose is also required. To allow better and faster solubilization of reagents, 10 equiv of citrate is finally added (Scheme 3). To avoid fouling and runaway fluids, the concentration of bismuth sodium citrate is optimized to 3 mM and the power to 25 W. In this case, for a concentration of 3 mM, the jump ΔpH, deduced from Equation 4, was observed for a $pH_{initial}$ of 12.2.

Scheme 3. Millifluidic Synthesis Conditions of Bismuth NPs Using Microwaves

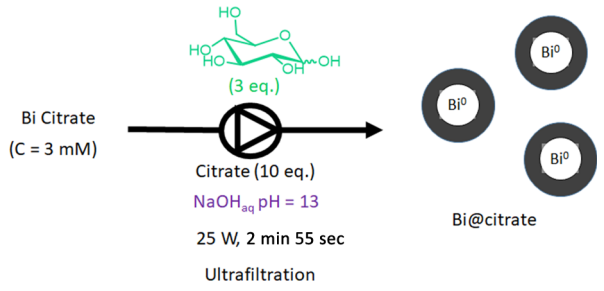

The influence of the flow rate and, therefore, the residence time was studied and bismuth NPs sizes were compared below (Table 7).

Table 7. Influence of the Flow Rate and Residence Time on Bismuth NPs Sizes

entry	flow rate	residence time	sizes (nm) in number (proportions %)	pH jump
1	1.0 mL/min	3 min 30 sec	64 ± 30 (100%)	complete
2	1.3 mL/min	2 min 55 sec	44 ± 16 (100%)	complete
3	1.5 mL/min	2 min 15 sec	131 ± 64 (71%) 46 ± 8 (29%)	complete
4	2.0 mL/min	1 min 45 sec	163 ± 68 (67%) 39 ± 8 (33%)	incomplete

When the flow rate was set at 1.0 mL/min, monodisperse bismuth NPs of about 64 ± 30 nm were obtained, but fouling (Table 7, entry 1) was observed in the tubing. For a flow rate greater than 1.5 mL/min, NPs were polydispersed and characterized by a bimodal size population (Table 7, entries 3 and 4). For a flow rate of 2 mL/min, the pH jump was incomplete; the residence time in the reactor was probably too low to ensure a total reduction (Table 7, entry 4). Finally, the optimal flow rate was reached at 1.3 mL/min. A complete pH jump was ensured, no fouling was observed, and monodisperse NPs with a size of 44 ± 16 nm were obtained (Table 7, entry 2).

Using these last conditions, we have confirmed the intra- and inter-operator reproducibility of bismuth NPs synthesis in our microwave millifluidic system (Table 8).

Table 8. Intra- and Inter-operator Reproducibility of Bismuth NPs Synthesis in Our Microwave Millifluidic System

operator	number of tests	average sizes (nm) in number (average proportions %)	pH jump	yield after ultrafiltration purification
A	3	38 ± 19 (100%)	complete	75%
B	3	52 ± 21 (100%)	complete	

The results presented in Table 8 demonstrated that this millifluidic synthesis coupled to ultrafiltration purification was reproducible with hydrodynamic sizes similar to those of the initial reaction (Table 7) and the pH jump was identical for each experiment (0.07). The yields were similar to those obtained in batch. However, the millifluidic system significantly improved the synthesis productivity to 96 mg/h of bismuth NPs (in comparison with 40 mg/h in batch). In a pre-industrial perspective, this productivity could be further improved by the increase in the number of microreactors to produce a parallel network.[70]

Characterizations of Bismuth NPs. Further characterizations of bismuth NPs obtained in batch (Table 6, entry 4) and the flow process (Table 7, entry 2) were performed below.

A TEM measure has given a mean diameter of 3 ± 1.0 nm (Figure S1) for bismuth NPs obtained under microwaves in batch. An identical size distribution was observed for homogeneous bismuth NPs obtained by flow chemistry coupled to microwaves (3 ± 1.3 nm) (Figure S1). The sizes obtained by TEM are much smaller than the hydrodynamic diameters measured by DLS at pH = 13 in batch (96 ± 37 nm (100%)) and in the flow process (44 ± 16 nm (100%)). The sizes obtained by DLS are usually bigger than those obtained by TEM.[71] TEM and DLS sizes often do not corroborate because DLS is an intensity-based technique and TEM is a number-based one, and moreover, DLS is very sensitive to the presence of reversible aggregation of nanoparticles in solution.[72] These differences are more limited in continuous flow probably due to the less formation of aggregates in solution.

For these bismuth NPs with a size distribution of 3 ± 1.0 nm (TEM), the XRD analysis is not usable due to broad

https://doi.org/10.1021/acssuschemeng.1c00396
ACS Sustainable Chem. Eng. 2021, 9, 9177−9187

peaks and low signal-to-noise ratios probably due to the small size of bismuth NPs, as recently commented in the literature on nanomaterials (Figure S3).[73]

The nature of bismuth NPs coating was determined by FT-IR and UV spectroscopy. Purified bismuth NPs were characterized by Fourier transform infrared (FT-IR) spectroscopy and compared to citrate molecules (Figure S2). A large band centered at 3415 cm^{-1} for the OH function on bismuth NPs showed the presence of citrate as an essential component of NPs coating. A significant shift from 3367 to 3415 cm^{-1} suggested a high association between citrate and the surface of bismuth NPs. Other major peaks such as C═O bands (1575 cm^{-1} (b) and 1582 cm^{-1} (c)) and C−O bands (1398 cm^{-1} (b) and 1396 cm^{-1} (c)) demonstrated the presence of citrate coated on the surface of bismuth NPs whatever the used process by comparison with the FT-IR spectrum of citrate.

UV spectroscopy has also confirmed the presence of citrate on the bismuth NPs surface (Figure S4) as the spectrum of our bismuth NPs was identical to that described in the literature by Fang et al.[74] The peak at 268 nm corresponds to the plasmonic band of bismuth NPs, which demonstrates the metallic structure of our bismuth NPs.

Finally, purified bismuth NPs were characterized by thermal gravimetric analysis (TGA) (Figure S5).

The TGA curve showed three losses of mass: one of them was centered on 50 °C corresponding to water (5−10%), and another was centered on 250 °C corresponding to citrate (5−12%) by analogy with citrate-coated gold nanoparticles.[39]

The surface density of citrate molecules adsorbed by the nanoparticle (n_{ligand}/nm^2) was quantified by thermogravimetry using the equation below (eq 5).

Calculation of $n_{citrate}$ by Nanoparticle

$$\frac{\text{weight percent of citrate (\%)}}{\text{weight percent of bismuth (\%)}} = \frac{n_{ligand} \times MW_{ligand}}{MW_{nanoparticle}} \quad (5)$$

where the molecular weight of the nanoparticle ($MW_{nanoparticle}$) was calculated *via* the following equation (eq 6a):

$$MW_{nanoparticle} = \rho \times N_A \times \frac{4}{3} \times \pi \times r^3_{nanoparticles} \quad (6a)$$

where N_A is the Avogadro number, ρ is the density of bismuth (9790 kg/m^3), and r is the radius of the nanoparticle (1.5 nm estimated by TEM). This calculation made it possible to obtain a value of a number of citrate molecules per nanoparticle (n_{ligand}) and then a surface density of ligand equal to 1 citrate per nm^2 for bismuth NPs obtained by batch and by the flow process. This surface density is directly dependent on the metal studied, nanoparticle size, pH of the colloidal solution, and chemical composition of the nanoparticle surface, as described in the literature.[75]

All of the FT-IR, UV, and TGA analyses have confirmed the production of citrate-coated bismuth NPs. Moreover, if we cluster all characterizations in the table below (Table 9), we observe that similar bismuth NPs were obtained in batch and in the continuous flow process. This showed our capability to produce these metallic nanoparticles in the 100 mg scale with our home-made millifluidic system under microwaves.

Table 9. Comparison of Data between Batch and Flow Chemistry Processes

characterization	batch process	flow chemistry process
hydrodynamic diameter (DLS)	96 ± 37 nm	44 ± 16 nm
size (TEM)	3 ± 1.0 nm	3 ± 1.3 nm
FT-IR	citrate coating	citrate coating
UV spectroscopy	citrate coating	citrate coating

CONCLUSIONS

The review of the literature[30] showed that no published bismuth NPs synthesis simultaneously respected all the principles of green nanochemistry.

In this work, we have designed a greener synthesis methodology that allowed reproducible access to bismuth NPs.

For that purpose, we have designed a synthesis that:

- Did not use an organic solvent but water as a green solvent.
- Used D-glucose as a nontoxic and feedstock renewable reducer.
- Used a sodium bismuth citrate precursor to maximize atom economy as the citrate counter-ion acted as a coating agent for the nanoparticle.
- Did not require a high energy input by using microwave heating.
- Reduced reaction time.
- Has limited waste reduction at the purification step by using ultrafiltration.
- Answered to an industrial challenge to use microwave activation to the scale-up.

D-Glucose as a reducing agent has never been described to our knowledge to obtain bismuth NPs. This reducing agent has made it possible to monitor the conversion of Bi(III) to Bi(0) by measuring the decrease in pH due to the reduction step. The monitoring of the conversion by pH-metry has never been previously demonstrated, to our knowledge, in NP synthesis.

All parameters of synthesis under microwave irradiation and purification have been optimized to study their influence on the size and distribution of nanoparticles. Our microwave batch synthesis and purification conditions allowed to produce monodisperse bismuth NPs with a DLS diameter of about 90 nm with very short reaction times (2 min 30 sec) (pH = 13). All the analytical characterizations have shown the obtaining of metallic bismuth NPs covered with citrate.

Finally, to increase the productivity of bismuth NPs synthesis and ensure an efficient scale-up, we have extrapolated our batch conditions (pH = 13) to a continuous millifluidic process.

To this end, we designed an experimental device coupling a HPLC pump and a Teflon reactor immersed in the microwave cavity.

After optimization of conditions, this process made it possible to increase the hourly productivity of nanoparticles by a factor of 16 (respectively 2.4) compared to the conventional thermal (respectively microwaves) heating batch process. This productivity could be further improved by the increase in the diameter of the tube, the flow rate and the number of microreactors to produce a parallel network.

This millifluidic system made it possible to obtain, after purification by ultrafiltration, bismuth NPs of smaller size (44

https://doi.org/10.1021/acssuschemeng.1c00396
ACS Sustainable Chem. Eng. 2021, 9, 9177−9187

nm in DLS) in comparison with the batch system. The intra- and inter-operator reproducibility of this millifluidic synthesis has been demonstrated and all analytical characterizations have shown the obtaining of bismuth NPs covered with citrate.

EXPERIMENTAL SECTION

Reagents. Bismuth citrate sodium (Alfa Aesar, >94%), D-glucose (Sigma, 99.5%), citric acid (Labosi, >98%), bismuth chloride (Acros, >99%), bismuth carbonate (Rectapur, 83%), bismuth nitrate pentahydrate (Acros, 98%), bismuth acetate (Alfa Aesar,>99%), bismuth citrate ammonium (Fluka >99%) and dithizone (TCI, >85%) were used in this study. All solutions were prepared using fresh, distillated H_2O.

Synthesis of Metallic Bismuth NPs in Batch by Thermal Activation. Bismuth citrate (1 equiv, 0.05 mmol, 20 mg) and D-glucose (1.7 equiv, 0.08 mmol, 16 mg) were solubilized in NaOH solution (1 M, 5 mL). The pH was measured (pH = 14) and the solution was heated to 120 °C during 2 h 30. At the end of the reaction, pH was again controlled and a pH jump was observed. The reaction mixture was acidified to pH 10 with a nitric acid solution (1 M). The nanoparticles were isolated by centrifugation at 4000 tr·min^{-1} (2.585 g) (Heraeus Primo centrifuges RCF, three washings with water at pH = 10 during 45 min, 30 min and 30 min). After purification, NPs were dispersed in water at pH = 10 and characterized by DLS.

Synthesis of Metallic Bismuth NPs in Batch under Microwave Irradiation. Bismuth citrate (1 equiv, 0.05 mmol, 20 mg) and D-glucose (1.7 eq, 0.08 mmol, 16 mg) were solubilized in NaOH solution (1 M, 5 mL). The pH was measured either pH = 14 or pH = 13 according to the experiment and the reaction was carried out under microwave irradiation (CEM Corporation, USA) at 75 W for 2 min 10 (pH = 14) or for 2 min 30 (pH = 13). At the end of the reaction, pH was again controlled and a pH jump was observed. The reaction mixture was acidified to pH 10 with a nitric acid solution (1 M). Ultrafiltration was performed on a 5 kDa cellulose filter (Merck) with a washing solution at pH = 10. The conductivity value of the filtrate was identical to those of washing water value (approximately 40 μS/cm). Purified NPs were dispersed in water at pH = 10 and characterized by DLS.

Synthesis of Metallic Bismuth NPs in Continuous Flow under Microwave Irradiation. In a conical flask, citric acid (10 equiv, 3 mmol, 570 mg) and bismuth citrate (1 equiv, 0.3 mmol, 120 mg) were dissolved in distilled water (76 mL). The pH was adjusted by using an aqueous solution of NaOH (5 M) to obtain a pH = 13 and a total volume of 80 mL. D-Glucose (3 equiv, 0.9 mmol, 162 mg) was added to the previous solution. The pH was measured and must be equal to 13. The solution was then pumped through the reactor by a HPLC pump (Waters, 600 controller). The flow reactor, made of 1/8 o.d. (0.32 cm) Teflon tubing, was irradiated under microwaves with a power of 25 W and the flow rate was set at 1.3 mL/min during 22 min. The flow controller (valve 3: conicity, 3°; 1 turn) installed at the end of Teflon tubing set the flow rate. The hot fluid was cooled in the tubing and collected in a flask. The crude was then purified by ultrafiltration (filtration membrane of 30 kDa, Merck) until the conductivity value of the filtrate was identical to those of the washing water value (approximately 40 μS/cm). After purification, NPs dispersed in water were characterized by DLS.

Characterizations of Bismuth Nanomaterials. Nanoparticles were analyzed by Fourier transform infrared (FT-IR) spectroscopy on a PerkinElmer Spectrum II equipped with a diffuse reflectance accessory. Two milligrams of nanoparticles was mixed with 10 mg of KBr. The spectra were recorded with a resolution of 2 cm^{-1} and with 64 scans. Dynamic light scattering (DLS) measurements were performed on a Malvern ZetaSizer ZEN3600 instrument equipped with a 633 nm laser (scattering angle, 175°) at 25 °C on a bismuth NPs solution (1 mM) diluted in water (RI, 1.33; viscosity, 0.8872). Three replicate measurements were performed by analysis in a cuvette ZEN0118 (200 μL). An instrumental algorithm was used to supply the hydrodynamic diameters as number distributions (bismuth RI, 2.145; absorption, 2.988). The measurements were presented with the average size of NPs ± standard deviation. Images were taken by transmission electron microscopy (TEM) on a Philips CM120 transmission electron microscope operating at 80 kV. Microscopy analyses were performed as follows: 200 μL droplets of the colloidal dispersion were cast onto formvar/carbon-coated copper grids (400 mesh) for a few minutes. From the TEM images, the bismuth NPs diameter distribution was determined from recorded images with ImageJ software version 1.48 (at least 300 counted particles). The measurements were presented with the average size of NPs ± standard deviation. Thermal stability and composition analyses (TGA) were carried out on a TGA Q500-type measuring instrument (TA Instruments, USA) under a nitrogen flow of 50 mL/min. The temperature was increased from 25 to 450 °C with a temperature gradient of 10 °C/min.

The coating agent number per nanoparticle was estimated by the next equation (eq 6), where the molecular weight of nanoparticles (MW) was estimated from:

Formula of Nanoparticles Molecular Weight

$$\mathrm{MW}_{\mathrm{nanoparticles}} = \rho \times N_A \times \frac{4}{3} \times \pi \times r^3{}_{\mathrm{nanoparticles}} \quad (6)$$

The UV−visible absorption spectra were collected using a Genesy 10UV scanning UV spectrometer (Thermo Spectronic) on a bismuth NPs solution (1 mM). The UV−visible calibration line was established with a growing concentration of bismuth NPs and a freshly prepared dithizone solution 0.01% (w/v) in ethanol (1 mL). To evaluate the bismuth yield, bismuth NPs (2 mg) were solubilized in a HCl solution (1 M, 5 mL). The reaction mixture was digested under microwave irradiation for 2 h at reflux. HCl solution (1 M, 5 mL) and distilled water (90 mL) were added to dilute the HCl solution (0.1 M, 100 mL). The solution absorbance was measured by UV−visible spectroscopy to evaluate the bismuth yield (eq 7).

Formula to Evaluate Bismuth Yield

$$N \times \frac{4}{3}\pi r^3{}_{\mathrm{sphere}} \times 0.524 = N_{\mathrm{A}} \times n\frac{4}{3}\pi r^3{}_{\mathrm{Bi}} \times \mathrm{yield} \quad (7)$$

where r_{sphere} is nanosphere radius; 0.524, compactness of a rhombohedral structure; N_A, Avogadro number; n, number of moles of bismuth atoms introduced via the precursor; r_{Bi}, atomic radius of bismuth (160 pm); and yield, yield valued by UV−visible spectroscopy.

ASSOCIATED CONTENT

Supporting Information

The Supporting Information is available free of charge at https://pubs.acs.org/doi/10.1021/acssuschemeng.1c00396.

TEM images of synthesized bismuth NPs under microwaves in batch and in continuous flow, FT-IR spectra, UV spectra and TGA curves of these bismuth NPs obtained under microwaves in batch and in continuous flow coupled to microwaves (PDF)

AUTHOR INFORMATION

Corresponding Authors

Catherine Gomez − *Laboratoire de Génomique, Bioinformatique et Chimie Moléculaire (EA 7528), Equipe de Chimie Moléculaire, Conservatoire National des Arts et Métiers (Cnam), HESAM Université, 75003 Paris, France;* orcid.org/0000-0002-3680-1235;
Email: catherine.gomez@lecnam.net

Marc Port − *Laboratoire de Génomique, Bioinformatique et Chimie Moléculaire (EA 7528), Equipe de Chimie Moléculaire, Conservatoire National des Arts et Métiers*

https://doi.org/10.1021/acssuschemeng.1c00396
ACS Sustainable Chem. Eng. 2021, 9, 9177−9187

(Cnam), HESAM Université, 75003 Paris, France; Email: marc.port@lecnam.net

Authors

Gauthier Hallot − *Laboratoire de Génomique, Bioinformatique et Chimie Moléculaire (EA 7528), Equipe de Chimie Moléculaire, Conservatoire National des Arts et Métiers (Cnam), HESAM Université, 75003 Paris, France*

Virginie Cagan − *Laboratoire de Génomique, Bioinformatique et Chimie Moléculaire (EA 7528), Equipe de Chimie Moléculaire, Conservatoire National des Arts et Métiers (Cnam), HESAM Université, 75003 Paris, France*

Sophie Laurent − *Laboratory of NMR and Molecular Imaging, University of Mons, B-7000 Mons, Belgium*

Complete contact information is available at: https://pubs.acs.org/10.1021/acssuschemeng.1c00396

Notes

The authors declare no competing financial interest.

■ ACKNOWLEDGMENTS

The authors thank the ministerial scholarship for the support of Gauthier Hallot's Ph.D. (ED406, Sorbonne University). They thank Matthieu Gervais (ENSAM, Paris) for his help in TGA analyses and Sophie Laurent (University of Mons) and Emilie Brun (University of Paris Saclay) for their help in TEM analyses. The present work has benefited from the Transmission Electron Microscopy facilities of Mons University and Imagerie-Gif (http://www.i2bc.parissaclay.fr/spip.php?article282). This core facility is a member of Infrastructures en Biologie Santé et Agronomie (IBiSA) and is supported by the French National Research Agency under Investments for the Future programs "France-BioImaging" and the Labex "Saclay Plant Science" (ANR-10-INSB-04-01 and ANR-11-IDEX-0003-02, respectively).

■ REFERENCES

(1) Smith, B. R.; Gambhir, S. S. Nanomaterials for In Vivo Imaging. *Chem. Rev.* **2017**, *117*, 901−986.

(2) Hutchison, J. E. The Road to Sustainable Nanotechnology: Challenges, Progress and Opportunities. *ACS Sustainable Chem. Eng.* **2016**, *4*, 5907−5914.

(3) Cinelli, M.; Coles, S. R.; Nadagouda, M.; Blaszczynski, J.; Slowinski, R.; Varma, R. S.; Kirwan, K. A Green Chemistry-Based Classification Model for the Synthesis of Silver Nanoparticles. *Green Chem.* **2015**, *17*, 2825−2839.

(4) Varma, R. S. Greener and Sustainable Trends in Synthesis of Organics and Nanomaterials. *ACS Sustainable Chem. Eng.* **2016**, *4*, 5866−5878.

(5) Wang, F.; Tang, R.; Yu, H.; Gibbons, P. C.; Buhro, W. E. Size- and shape-controlled synthesis of bismuth nanoparticles. *Chem. Mater.* **2008**, *20*, 3656−3662.

(6) Wang, J.; Wang, X.; Peng, Q.; Li, Y. Synthesis and characterization of bismuth single-crystalline nanowires and nanospheres. *Inorg. Chem.* **2004**, *43*, 7552−7556.

(7) Xia, F.; Xu, X.; Li, X.; Zhang, L.; Zhang, L.; Qiu, H.; Wang, W.; Liu, Y.; Gao, J. Preparation of Bismuth Nanoparticles in Aqueous Solution and Its Catalytic Performance for the Reduction of 4-Nitrophenol. *Ind. Eng. Chem. Res.* **2014**, *53*, 10576−10582.

(8) Cui, Z.; Zhang, Y.; Li, S.; Ge, S. Preparation and photocatalytic performance of Bi nanoparticles by microwave-assisted method using ascorbic acid as reducing agent. *Catal. Commun.* **2015**, *72*, 97−100.

(9) Shahbazi, M. A.; Faghfouri, L.; Ferreira, M. P. A.; Figueiredo, P.; Maleki, H.; Sefat, F.; Hirvonen, J.; Santos, H. A. The versatile biomedical applications of bismuth-based nanoparticles and composites: therapeutic, diagnostic, biosensing, and regenerative properties. *Chem. Soc. Rev.* **2020**, *49*, 1253−1321.

(10) Lusic, H.; Grinsta, M. W. X-Ray-Computed Tomography Contrast Agents. *Chem. Rev.* **2013**, *113*, 1641.

(11) Brown, A. L.; Naha, P. C.; Benavides-Montes, V.; Litt, H. I.; Goforth, A. M.; Cormode, D. P. Synthesis, X - Ray Opacity, and Biological Compatibility of Ultra-High Payload Elemental Bismuth Nanoparticle X - Ray Contrast Agents. *Chem. Mater.* **2014**, *26*, 2266−2274.

(12) Wei, B.; Zhang, X.; Zhang, C.; Jiang, Y.; Fu, Y. Y.; Yu, C.; Sun, S. K.; Yan, X. P. Facile Synthesis of Uniform-Sized Bismuth Nanoparticles for CT Visualization of Gastrointestinal Tract in Vivo. *ACS Appl. Mater. Interfaces* **2016**, *8*, 12720−12726.

(13) Chakravarty, S.; Unold, J.; Shuboni-mulligan, D. D.; Blanco-fernandez, B.; Shapiro, E. M. Surface Engineering of Bismuth Nanocrystals to Counter Dissolution. *Nanoscale* **2016**, *8*, 13217−13222.

(14) Swy, E. R.; Schwartz-Duval, A. S.; Shuboni, D. D.; Latourette, M. T.; Mallet, C. L.; Parys, M.; Cormode, D. P.; Shapiro, E. M. Dual-Modality, Fluorescent, PLGA Encapsulated Bismuth Nanoparticles for Molecular and Cellular Fluorescence Imaging and Computed Tomography. *Nanoscale* **2014**, *6*, 13104−13112.

(15) Li, Z.; Liu, J.; Hu, Y.; Li, Z.; Fan, X.; Sun, Y.; Besenbacher, F.; Chen, C.; Yu, M. Biocompatible PEGylated Bismuth Nanocrystals: " All-in-One " Theranostic Agent with Triple-Modal Imaging and Efficient in Vivo Photothermal Ablation of Tumors. *Biomaterials* **2017**, *141*, 284−295.

(16) Yu, X.; Li, A.; Zhao, C.; Yang, K.; Chen, X.; Li, W. Ultrasmall Semimetal Nanoparticles of Bismuth for Dual-Modal Computed Tomography/Photoacoustic Imaging and Synergistic Thermoradiotherapy. *ACS Nano* **2017**, *11*, 3990−4001.

(17) Yang, S.; Li, Z.; Wang, Y.; Fan, X.; Miao, Z.; Hu, Y.; Li, Z.; Sun, Y.; Besenbacher, F.; Yu, M. Multifunctional Bi@PPy-PEG Core−Shell Nanohybrids for Dual-Modal Imaging and Photothermal Therapy. *ACS Appl. Mater. Interfaces* **2018**, *10*, 1605−1615.

(18) Yang, C.; Guo, C.; Guo, W.; Zhao, X.; Liu, S.; Han, X. Multifunctional Bismuth Nanoparticles as Theranostic Agent for PA/CT Imaging and NIR Laser-Driven Photothermal Therapy. *ACS Appl. Mater. Interfaces* **2018**, *1*, 820−830.

(19) Liu, Y.; Zhang, P.; Li, F.; Jin, X.; Li, J.; Chen, W.; Li, Q. Metal-based NanoEnhancers for Future Radiotherapy: Radiosensitizing and Synergistic Effects on Tumor Cells. *Theranostics* **2018**, *8*, 1824−1849.

(20) Hossain, M.; Su, M. Nanoparticle Location and Material Dependent Dose Enhancement in X-Ray Radiation Therapy. *J. Phys. Chem. C. Nanomater. Interfaces* **2012**, *116*, 23047−23052.

(21) Hossain, M.; Luo, Y.; Sun, Z.; Wang, C.; Zhang, M.; Fu, H.; Qiao, Y.; Su, M. X-Ray Enabled Detection and Eradication of Circulating Tumor Cells with Nanoparticles. *Biosens. Bioelectron.* **2012**, *38*, 348−354.

(22) Deng, J.; Xu, S.; Hu, W.; Xun, X.; Zheng, L.; Su, M. Tumor Targeted, Stealthy and Degradable Bismuth Nanoparticles for Enhanced X-Ray Radiation Therapy of Breast Cancer. *Biomaterials* **2018**, *154*, 24−33.

(23) Jiao, L.; Li, Q.; Deng, J.; Okosi, N.; Xia, J.; Su, M. Nanocellulose Templated Growth of Ultra-Small Bismuth Nanoparticles for Enhanced Radiation Therapy. *Nanoscale* **2018**, *10*, 6751−6757.

(24) Yu, N.; Wang, Z.; Zhang, J.; Liu, Z.; Zhu, B.; Yu, J.; Zhu, M.; Peng, C.; Chen, Z. Thiol-Capped Bi Nanoparticles as Stable and All-in-One Type Theranostic Nanoagents for Tumor Imaging and Thermoradiotherapy. *Biomaterials* **2018**, *161*, 279−291.

(25) Luo, Y.; Hossain, M.; Wang, C.; Qiao, Y.; An, J.; Ma, L.; Su, M. Targeted Nanoparticles for Enhanced X-Ray Radiation Killing of Multidrug-Resistant Bacteria. *Nanoscale* **2013**, *5*, 687−694.

(26) Lei, P.; An, R.; Zhang, P.; Yao, S.; Song, S.; Dong, L.; Xu, X.; Du, K.; Feng, J. Ultrafast Synthesis of Ultrasmall Poly (Vinylpyrrolidone) - Protected Bismuth Nanodots as a Multifunctional Theranostic Agent for In Vivo Dual-Modal CT / Photothermal-

Imaging-Guided Photothermal Therapy. *Adv. Funct. Mater.* **2017**, *27*, 1702018−1702010.
(27) Lu, S.; Xu, D.; Liao, R.; Luo, J.; Liu, Y.; Qi, Z.; Zhang, C.; Ye, N.; Wu, B.; Xu, H. Single-Component Bismuth Nanoparticles as a Theranostic Agent for Multimodal Imaging-Guided Glioma Therapy. *Comput. Struct. Biotechnol. J.* **2019**, *17*, 619−627.
(28) Gomez, C.; Hallot, G.; Pastor, A.; Laurent, S.; Brun, E.; Sicard-Roselli, C.; Port, M. Metallic Bismuth Nanoparticles: Towards a Robust, Productive and Ultrasound Assisted Synthesis from Batch to Flow-Continuous Chemistry. *Ultrason. Sonochem.* **2019**, *56*, 167−173.
(29) Gomez, C.; Port, M.; Hallot, G. Bismuth Metallic (0) Nanoparticles, Process of Manufacturing and Uses Thereof. EP Pat., 18 305 851.0, 2018.
(30) Gomez, C.; Hallot, G.; Port, M. *Bismuth metallic nanoparticles in Grumezescu, A.M. Inorganic frameworks as smart nanomedicines. Pharmaceutical Nanotechnology Series*; ed. Elsevier: 2018, *17020181*−699.
(31) Kundu, S.; Wang, K.; Liang, H. Size-controlled synthesis and self-assembly of silver nanoparticles within a minute using microwave irradiation. *J. Phys. Chem. C* **2009**, *113*, 134−5141.
(32) Pal, A.; Shah, S.; Devi, S. Synthesis of Au, Ag and Au-Ag alloy nanoparticles in aqueous polymer solution. *Colloids Surf., A* **2007**, *302*, 51−57.
(33) Mallikarjuna, N. N.; Varma, R. S. Microwave-Assisted Shape-Controlled Bulk Synthesis of Noble Nanocrystals and Their Catalytic Properties. *Cryst. Growth Des.* **2007**, *7*, 686−690.
(34) Uppal, M. A.; Kafizas, A.; Ewing, M. B.; Parkin, I. P. The effect of initiation method on the size, monodispersity and shape of gold nanoparticles formed by the Turkevich method. *New J. Chem.* **2010**, *34*, 2906−2914.
(35) Anastas, P. T.; Zimmerman, J. B. Peer Reviewed: Design Through the 12 Principles of Green Engineering. Sustainability requires objectives at the molecular, product, process, and system levels. *Environ. Sci. Technol.* **2003**, *37*, 94A−101A.
(36) Vaccaro, L. *Sustainable Flow Chemistry: Methods and Applications*; ed. Wiley: 2017, 1−317, DOI: 10.1002/9783527689118
(37) Eastman, H. E.; Jamieson, C.; Watson, A. J. B. Development of Solvent Selection Guides. *Aldrichimica Acta* **2015**, *48*, 51−55.
(38) *ICH steering committee. Impurities: Guideline for Residual Solvent*; http://www.ich.org/fileadmin/Public_Web_Site/ICH_Products/Guidelines/Quality/Q3C/Q3C_R6__Step_2.
(39) Chen, S.; Kimura, K. Synthesis and Characterization of Carboxylate-Modified Gold Nanoparticle Powders Dispersible in Water. *Langmuir* **1999**, *15*, 1075−1082.
(40) Liu, J.; Qin, G.; Raveendran, P.; Ikushima, Y. Facile "Green" Synthesis, Characterization, and Catalytic Function of β-D-Glucose-Stabilized Au Nanocrystals. *Chem. − Eur. J.* **2006**, *12*, 2131−2138.
(41) Morgunov, I. G.; Kamzolova, S. V.; Lunina, J. N. Citric Acid Production by Yarrowia lipolytica Yeast on Different Renawable Raw Materials. *Fermentation* **2018**, *4*, 1−7.
(42) Kharissova, O. V.; Osorio, M.; Garza, M.; Kharisov, B. I. Study of Bismuth Nanoparticles and Nanotubes Obtained by Microwave Heating. *Synth. React. Inorg. M.* **2008**, *38*, 567−572.
(43) Bilecka, I.; Niederberger, M. Microwave chemistry for inorganic nanomaterials synthesis. *Nanoscale* **2010**, *2*, 1358−1374.
(44) Zhu, Y. J.; Chen, F. Microwave-Assisted Preparation of Inorganic Nanostructures in Liquid Phase. *Chem. Rev.* **2014**, *114*, 6462−6555.
(45) Raveendran, P.; Fu, J.; Wallen, S. L. A simple and "green" method for the synthesis of Au, Ag and Au-Ag alloy nanoparticles. *Green Chem.* **2006**, *8*, 34−38.
(46) Shahbazali, E.; Hessel, V.; Noël, T.; Wang, Q. Metallic Nanoparticles Made in Flow and Their Catalytic Applications in Organic Synthesis. *Nanotechnol. Rev.* **2014**, *3*, 65−86.
(47) Tsuji, M.; Hashimoto, M.; Nishizawa, Y.; Kubokawa, M.; Tsuji, T. Microwave-Assisted Synthesis of Metallic Nanostructures in Solution. *Chem. Eur. J.* **2005**, *11*, 440−452.
(48) Baghbanzadeh, M.; Carbone, L.; Cozzoli, P. D.; Kappe, C. O. Microwave-Assisted Synthesis of Colloidal Inorganic Nanocrystals. *Angew. Chem. Int. Ed.* **2011**, *50*, 11312−11359.
(49) Kappe, C. O. Controlled Microwave Heating in Modern Organic Synthesis. *Angew. Chem. Int. Ed.* **2004**, *43*, 6250−6284.
(50) Nadagouda, M. N.; Speth, T. F.; Varma, R. S. Microwave-Assisted Green Synthesis of Silver Nanostructures. *Acc. Chem. Res.* **2011**, *44*, 469−478.
(51) Seol, S. K.; Kim, D.; Jung, S.; Hwu, Y. Microwave synthesis of gold nanoparticles: Effect of applied microwave power and solution pH. *Mater. Chem. Phys.* **2011**, *131*, 331−335.
(52) Polshettiwar, V.; Nadagouda, M. N.; Varma, R. S. Microwave-Assisted Chemistry: a Rapid and Sustainable Route to Synthesis of Organics and Nanomaterials. *Aust. J. Chem.* **2009**, *62*, 16−26.
(53) Gerbec, J. A.; Magana, D.; Washington, A.; Strouse, G. F. Microwave-Enhanced Reaction Rates for Nanoparticle Synthesis. *J. Am. Chem. Soc.* **2005**, *127*, 15791−15800.
(54) Hu, B.; Wang, S. B.; Wang, K.; Zhang, M.; Yu, S. H. Microwave-Assisted Rapid Facile "Green" Synthesis of Uniform Silver Nanoparticles: Self-Assembly into Multilayered Films and Their Optical Properties. *J. Phys. Chem. C* **2008**, *112*, 11169−11174.
(55) Liu, F. K.; Ker, C. J.; Chang, Y. C.; Ko, F. H.; Chu, T. C.; Dai, B. T. Microwave Heating for the Preparation of Nanometer Gold Particles. *Jpn. J. Appl. Phys.* **2003**, *42*, 4152−4158.
(56) Wu, J.; Yang, H.; Li, H.; Lu, Z.; Yu, X.; Chen, R. Microwave synthesis of bismuth nanospheres using bismuth citrate as a precursor. *J. Alloys Compd.* **2010**, *498*, L8−L11.
(57) Estrada Flores, M.; Santiago Jacinto, P.; Reza San Germán, C. M.; Rendón Vázquez, L.; Borja Urby, R.; Cayetano Castro, N. Surfactant-Free Synthesis of Metallic Bismuth Spheres by Microwave-Assisted Solvothermal Approach as a Function of the Power Level. *Front. Mater. Sci.* **2016**, *10*, 394−404.
(58) Safardoust-Hojaghan, H.; Salavati-Niasari, M.; Hassan Motaghedifard, M.; Mostafa Hosseinpour-Mashkani, S. Synthesis of Micro Sphere-like Bismuth Nanoparticles by Microwave Assisted Polyol Method; Designing a Novel Electrochemical Nanosensor for Ultra-Trace Measurement of Pb^{2+} Ions. *New J. Chem.* **2015**, *39*, 4676−4684.
(59) Nishioka, M.; Miyakawa, M.; Kataoka, H.; Koda, H.; Sato, K.; Suzuki, T. M. Continuous Synthesis of Monodispersed Silver Nanoparticles Using a Homogeneous Heating Microwave Reactor System. *Nanoscale* **2011**, *3*, 2621−2626.
(60) Horikoshi, S.; Abe, H.; Torigoe, K.; Abe, M.; Serpone, N. Access to Small Size Distributions of Nanoparticles by Microwave-Assisted Synthesis. Formation of Ag Nanoparticles in Aqueous Carboxymethylcellulose Solutions in Batch and Continuous-Flow Reactors. *Nanoscale* **2010**, *2*, 1441−1447.
(61) Dzido, G.; Markowski, P.; Małachowska-Jutsz, A.; Prusik, K.; Jarzębski, A. B. Rapid Continuous Microwave-Assisted Synthesis of Silver Nanoparticles to Achieve Very High Productivity and Full Yield: From Mechanistic Study to Optimal Fabrication Strategy. *J. Nanopart. Res.* **2015**, *17*, 27−15.
(62) Harada, M.; Cong, C. Microwave-Assisted Polyol Synthesis of Polymer-Protected Monometallic Nanoparticles Prepared in Batch and Continuous-Flow Processing. *Ind. Eng. Chem. Res.* **2016**, *55*, 5634−5643.
(63) Bayazit, M. K.; Yue, J.; Cao, E.; Gavriilidis, A.; Tang, J. Controllable Synthesis of Gold Nanoparticles in Aqueous Solution by Microwave Assisted Flow Chemistry. *ACS Sustainable Chem. Eng.* **2016**, *4*, 6435−6442.
(64) Estel, L.; Poux, M.; Benamara, N.; Polaert, I. Continuous flow-microwave reactor: Where are we? *Chem. Eng. Process.* **2017**, *113*, 56−64.
(65) Chatel, G.; Varma, R. S. Ultrasound and microwave irradiation: contributions of alternative physicochemical activation methods to Green Chemistry. *Green Chem.* **2019**, *21*, 6043−6050.
(66) Vaccaro, L.; Lanari, D.; Marrocchia, A.; Strappaveccia, G. Flow approaches towards sustainability. *Green Chem.* **2014**, *16*, 3680−3704.

https://doi.org/10.1021/acssuschemeng.1c00396
ACS Sustainable Chem. Eng. 2021, 9, 9177−9187

(67) Movsisyan, M.; Delbeke, E. P. I.; Berton, J. K. E. T.; Battilocchio, C.; Ley, S. V.; Stevens, C. V. Taming hazardous chemistry by continuous flow technology. *Chem. Soc. Rev.* **2016**, *45*, 4892−4928.
(68) Lobet, O.; Vizza, A. SiC Advanced-Flow Reactors for Highly Corrosive Media. *Spec. Chem. Mag.* **2016**, *36*, 32−35.
(69) Garagalza, O. Polymérisation Radicalaire En Continu Dans Un Systeme Millifluidique Assistée Par Micro-Ondes. *Univ. PAU des Pays l'Adour* **2013**, 1−192.
(70) Haswell, S. J.; Watts, P. Green chemistry: synthesis in micro reactors. *Green Chem.* **2003**, *5*, 240−249.
(71) Shaterabadi, Z.; Nabiyuni, G.; Soleymani, M. High impact of *in situ* dextran coating on biocompatibility, stability and magnetic properties of iron oxide nanoparticles. *Mater. Sci. Eng. C* **2017**, *75*, 947−956.
(72) Bhattacharjee, S. DLS and zeta potential − What they are and what they are not ? *J. Controlled Release* **2016**, *235*, 337−351.
(73) Holder, C. F.; Schaak, R. E. Tutorial on Powder X-ray Diffraction for Characterizing Nanoscale Materials. *ACS Nano* **2019**, *13*, 7359−7365.
(74) Fang, J.; Stokes, K. L.; Wiemann, J. A.; Zhou, W. L.; Dai, J.; Chen, F.; O'Connor, C. J. Microemulsion-Processed Bismuth Nanoparticles. *Mater. Sci. Eng., B* **2001**, *83*, 254−257.
(75) Bajaj, M.; Wangoo, N.; Jain, D. V. S.; Sharma, R. K. Quantification of adsorbed and dangling citrate ions on gold nanoparticle surface using thermogravimetric analysis. *Sci. Rep.* **2020**, 8213−8220.

https://doi.org/10.1021/acssuschemeng.1c00396
ACS Sustainable Chem. Eng. 2021, 9, 9177−9187